CSSA

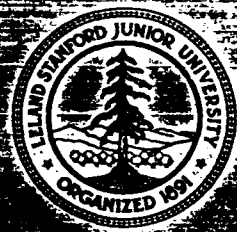## SPECTRAL ANALYSIS
OF THE ELATINA VARVE SERIES

R.N. Bracewell

Space, Telecommunications
and Radioscience Laboratory

CSSA-ASTRO-88-13
February 1988

CENTER FOR SPACE SCIENCE AND ASTROPHYSICS
STANFORD UNIVERSITY
Stanford, California

DTIC
SELECTE
AUG 1988

SPECTRAL ANALYSIS
OF THE ELATINA VARVE SERIES

R.N. Bracewell

Space, Telecommunications
and Radioscience Laboratory

DTIC
S ELECTE D
AUG 3 1 1988
H

SPECTRAL ANALYSIS OF THE ELATINA VARVE SERIES

R.N. Bracewell

Space, Telecommunications and Radioscience Laboratory, Stanford, California 94305-4035, U.S.A.

Abstract. The Elatina formation in South Australia, which provides a rich fossil record of presumptive solar activity in the late Precambrian, is of great potential significance for the physics of the sun because it contains laminae grouped in cycles of about 12, an appearance suggestive of the solar cycle. The actual spectrum of the lamina-thickness series is rather complex, 20 or more spectral lines having been recognized by Fourier analysis. It is shown how these numerous lines arise as combination frequencies, from a much simpler intrinsic spectrum, by rectification. Optical studies of the sun have shown that there is a magnetic polarity reversal on the sun every 11 years approximately, but terrestrial consequences of solar activity, for example in the ozonosphere or ionosphere, do not respond to solar magnetism; thus the negative-going semicycles of the full magnetic cycle are in effect rectified. Application of this knowledge to the Elatina formation shows that derectification simplifies the spectrum of the lamina-thickness series in exactly the way that one would expect if the solar cycle were at work here also. Zig-zag effect, an alternation of cycle thickness, is taken to be due, not to a beat phenomenon, but to rectification in the presence of a weak 345-year oscillation; subtraction of this oscillation after derectification is essential to the simplifying procedure. The fundamental period is established at a new sharper value of 23.7 ± 0.2 years as compared with the looser 22.2 ± 1.8 years for the modern sunspot series. This paper treats the laminae as varves laid down yearly and modulated in thickness in accordance with the late Precambrian sunspot activity for the year of deposition. Since the difference between 23.7 and 22.2 is less than a standard deviation it is premature to speculate that the sunspot cycle period has undergone secular change: indeed the possibility that the solar oscillator has been secularly stable is not ruled out. The high Q now demonstrated for the varve oscillator (around 120 compared with a previous value of 12) weakens support for that part of solar dynamo theory that ascribes the solar cycle to a self-sustaining relaxation oscillation; conversely, the evidence for an internal solar clock mechanism is strengthened. A wave propagation zone intervening between the clock and the solar surface could produce the intrinsic spectrum.

1. Introduction

Sedimentary laminae of light-coloured silt or fine sand in a dark clay matrix, found in the 680 million year old Elatina formation at Pichi Richi pass, South Australia, contain a record that has been interpreted as annual solar activity in late Precambrian time (Williams 1981, 1983, 1985, 1986, 1987; Williams and Tonkins 1985). This paper is one of a series (Bracewell, 1985, 1986c, 1988a,b,c, Bracewell and Williams 1986) stimulated by the varve interpretation. Figure 1 presents the varve-thickness series for 1337 years that has been studied in previous papers (Williams, 1985; Williams and Sonett, 1985; Bracewell and Williams, 1986; Sonett and Williams, 1987; Bracewell, 1988a). In this informative but complicated graph of the actual data one sees principal peaks P_1 of the Elatina cycle spaced 314 years, subsidiary peaks P_2, and episodes of antiphased zig-zag effect (alternating peak value) at A and B. Zig-zag effect presents itself to the eye as an alternation in thickness of the groups of about 12 laminae composing the cycles that are identified with the solar cycle under the varve interpretation. An alternative interpretation offered by Zahnle and Walker (1987) ascribes zig-zag effect to tidal influence but cannot apply to the Elatina formation because the two-frequency beat mechanism proposed calls for pronounced modulation of the thinnest laminae of each cycle.

Following a preliminary study (Williams, 1985), more detailed spectral analysis of the 1337 varves was carried out by Sonett and Williams (1987), who, in a major investigation, not only obtained the discrete Fourier transform but also a maximum entropy estimate of the spectrum, a least-squares periodogram, and a comparison between the two halves of the sequence. Table I summarizes the frequencies, periods and amplitudes of the 40 spectral peaks recorded in their Tables IIa and IIb. For ease of comparison with the present paper, the amplitudes presented are the square roots of the original power spectral densities, normalized to make the largest value equal to 100. Fig. 2(a) shows the spectral lines from Table I, those from the upper half of the varve sequence being drawn upward and those for the lower half downward.
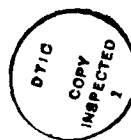
Clearly the actual spectrum is a complex one that is not easy to absorb. The purpose of this paper is to present a simpler structure, or intrinsic spectrum [Figure 2(b)] that will be uncovered by appropriate data analysis.

TABLE I

Spectral peaks found in the upper and lower halves of the varve-thickness series by Sonett and Williams (1987).

Upper half			Lower half		
Frequency c/a	Period yr	Amplitude	Frequency c/a	Period yr	Amplitude
0.003	334	73	0.003	332	87
0.006	167	67	0.006	165	51
0.010	99.2	19	0.011	88.3	32
0.016	62	8	0.036	27.9	22
0.026	38.7	6	0.039	25.6	38
0.033	30.7	19	0.042	23.9	35
0.039	25.7	51	0.045	22.3	40
0.041	24.3	17	0.048	21	16
0.045	22.3	59	0.051	19.6	17
0.048	20.9	13	0.055	18.0	17
0.051	19.6	31	0.058	17.2	16
0.062	16.2	8	0.061	16.3	22
0.065	15.4	14	0.065	15.4	15
0.073	13.8	35	0.068	14.7	29
0.077	13.0	67	0.070	14.2	41
0.081	12.4	56	0.075	13.4	51
0.084	11.9	100	0.081	12.4	98
0.087	11.5	42	0.084	11.9	80
0.090	11.1	88	0.090	11.1	79
0.097	10.3	46	0.096	10.4	52

WHITE OUT CENTER

3

2. The Centralized Series $C(t)$ and the Modulation Envelope

Among phenomena that are apparent from Figure 1 is a pronounced modulation of the layer thickness, referred to as the Elatina cycle, that has a period T_E of about 314 years. The modulation envelope was extracted by Williams (1983, 1985), and redetermined by Bracewell and Williams (1986) as follows. The varve series that gives the thickness $V(t)$ in μm of the varve for year t was first derectified to yield the alternating series $V_\pm(t)$ defined by

$$V(t) = V_0 + \mid V_\pm(t) \mid .$$

In this equation V_0 is a numerically determinate threshold of 70 μm interpretable as the thickness of silt that would be deposited in a year when the sunspot number was zero. After V_0 was subtracted from $V(t)$, the sign of the difference was reversed at the times t_j of minima and the value $V_\pm(t_j)$ was put to zero. In appropriate cases the sign reversal was taken between years.

Interpretation of zig-zag effect. A key feature of the present procedure is the removal of zig-zag or sawtooth effect (Williams, 1985). It had been mentioned (Williams, 1985) that the sawtooth pattern (a line-segment graph of cycle thickness versus cycle number) is mathematically describable as a beat between two oscillations with periods near 24 years. Sonett and Williams (1985) suggested that a beat between periods 22.4 and 25.8 years might be responsible, but examination of Figure 2(a) warns that the two periods mentioned be taken in context. When all the components of the full 24-year multiplet beat together the result is a waveform not possessing the necks that Williams (1985) described.

The interpretation (Bracewell, 1985) of sawtooth effect to be adopted here is illustrated in Figure 3. The upper part shows an oscillation of short period T_M (representing the magnetic cycle) superimposed on a weaker oscillation of (longer) period $T_U = 345$ years; when the composite waveform is rectified (lower part) a double-branched upper envelope is produced within which zig-zag effect is seen. The double upper envelope crosses itself (or passes through necks N) at intervals $T_U/2$, and at each such neck the phase of the zig-zag effect reverses by $180°$. This elementary explanation of zig-zag effect shows that the upper envelope of the example has two sinusoidal branches that intersect, and that the rectified waveform, representing varve thickness, rises up from a single-valued level base to the double-valued upper envelope, rising alternately to each branch.

A two-element beat pattern [such as $a_1 \sin(2\pi t/22.4) + a_2 \sin(2\pi t/25.8)$] does not rise from a defined base level but shuttles quasisinusoidally back and forth between a double upper envelope and a lower envelope that is not level and is also double-valued. The envelopes are not sinusoidal and do not intersect, unless $a_1 = a_2$.

4

When one sums the full multiplet $\Sigma a_i \sin(2\pi t / P_i)$ comprising approximately seven components with amplitude a_i and period P_i around 24 years, the resultant sum describes the Elatina cycle, as to amplitude, and through modulation of the times of zero crossing expresses phase and frequency modulation associated with the Elatina cycle. Thus, beats between two adjacent frequencies are not the source of the zig-zag effect.

An explanation of zig-zag effect in terms of a beat between two sinusoids given by Zahnle and Walker (1987) in support of a lunar theory of the Elatina varves also fails to reproduce the single-valued level lower envelope and therefore cannot be correct. The present paper takes zig-zag effect as evidence for the existence of a weak long period oscillation $U(t)$ of period T_U, to be referred to as the Elatina undulation.

Derivation of the centralized series. After derectification. the Elatina undulation $U(t)$, which has a period T_U of approximately 345 years, was determined with the use of a specific low-pass filter and subtracted from $V_\pm(t)$ to establish a centralized undulation-free oscillation $C(t)$. Thus

$$C(t) = V_\pm(t) - U(t).$$

The preparation of the data makes $C(t)$, shown in Figure 4, easier to assimilate than the graph of $V(t)$ in Figure 1. As a further aid to comprehension. the starting points of the four segments shown advance 314 years at a time. Not only is the modulation envelope much more apparent to the eye, but so is the degree of repeatability. Adjacent semicycles with contrasting shapes are conspicuous; the sharp negative semicycles at years 62 and 85 result from a near coincidence of a maximum of the Elatina cycle with a negative maximum of the undulation. The nonlinearity described in earlier papers (e.g. Bracewell, 1988b) acts to produce successive sharp and blunt semicycles. Variations in semicycle duration are also easily seen.

Elatina cycle envelope. Summing the absolute values of $C(t)$ over a double cycle (the varve equivalent of the solar magnetic cycle), i.e. from each t_j to t_{j+2}, gave a modulation envelope (Figure 5) that essentially confirmed the earlier description given by Williams (1983, 1985). This envelope method, apart from the data conditioning, is related to an envelope method described by Dicke (1978).

The shape of the modulation envelope is not simple; it exhibits a principal peak $P1$ at year 60, a secondary peak $P2$ at year 278 of relative strength about 0.6, a broad, principal minimum $M1$ at year 181 that descends to about 0.4 of the peak value at $P1$, and a narrow secondary minimum $M2$ at year 3 that descends to about 0.5 of $P1$. In addition there is a weak but noticeable wiggle W between $P1$ and $M1$ at about year 102.

Fourier analysis of the averaged envelope $E_E(t)$ gives the results shown in Table II for the coefficients a_n, b_n, c_n defined by

$$E_E(t) = 1 + \sum \left[a_n \cos(\frac{2\pi nt}{T_E}) + b_n \sin(\frac{2\pi nt}{T_E}) \right]$$

and $c_n = \sqrt{a_n^2 + b_n^2}$. The time origin is chosen so that the principal peak P_1 is at year 60 in Figure 5, corresponding to regularly spaced varve years 60, 374, 688, 1002 and 1316 in Figure 1.

TABLE II

Fourier coefficients for the Elatina modulation envelope $E_E(t)$.

n	1	2	3	4	5	6	7
a_n	0.133	−0.190	−0.099	−0.034	0.022	0.008	0.002
b_n	0.331	−0.007	−0.052	−0.064	−0.019	0.009	0.008
c_n	0.356	0.190	0.112	0.072	0.029	0.013	0.008

3. Spectral Analysis

The centralized undulation-free series C(t) was extended with trailing zeros to a length of 2048 elements and Fourier analyzed by means of the Hartley transform (Bracewell, 1986b). The result is shown in Figure 6. There is a fundamental band around a 24-year period and a noticeable 8-year third harmonic band. There is no zero-frequency component and little at the second harmonic (period 12 years). However, the fundamental contains a series of sidebands reflecting the known spectrum of the modulation envelope.

If one added the 345-year undulation back into $C(t)$, and rectified, and then performed a Fourier analysis of $| C(t) + U(t) |$ a very much more complicated spectrum would result that included a long series of harmonics of a 12-year fundamental with sidebands, harmonics of a 172.5-year fundamental, a band extending from zero frequency, and numerous sum and difference frequencies. This complicated spectrum is essentially the one determined by Sonett and Williams (1987). Many of the lines of the complicated spectrum are simply artefacts of rectification and are without independent importance; conversely, the third harmonic, which is important, is cancelled out by rectification, and does not appear in the Sonett and Williams spectrum (which will be referred to as the actual spectrum), because its sign is reversed at 1.5 cycle intervals. As a matter of history, the third harmonic was discovered in connection with sunspots by Cole (1973), who was the first to apply the concept of derectification (Bracewell 1953) to Fourier analysis of the sunspot number series.

Clearly the spectrum of Figure 6 describes the data rather economically. A detailed discussion is given in Section 6; meanwhile the principal spectral peaks of $C(t)$ in the frequency range from zero to 0.1 c/a are shown in Table III and have been graphed in Figure 2(b).

The line at 345 yr is not part of the spectrum of $C(t)$, but has been indicated for reference. Application of the idea of derectification shows that all the previously reported spectral lines derive from a much simpler intrinsic spectrum comprising (a) a 23.7-year carrier accompanied by a few sidebands associated with the 314-year Elatina amplitude modulation and (b) a weak line at 345 years. That all the detail should be explicable in terms of derectification was inevitable; what was not inevitable is that the new description should prove to be notably simple. a result that confirms the physical significance of this unravelment.

TABLE III

Spectral peaks of $C(t)$.

Frequency c/a	Period yr	Amplitude
0.029	34.1	11
0.033	30.6	14
0.036	28.1	16
0.039	25.6	56
0.042	23.8	100
0.045	22.0	20
0.048	20.7	46
0.052	19.3	10
0.055	18.1	10

If the spectrum of $C(t)$ in Figure 6 is compared with Figure 2(a), it will be seen that the content of the frequency band from zero to 0.02 c/a has disappeared as a direct result of derectification. There is nothing in $C(t)$ at 345 years, or submultiples, because the undulation was removed in advance. The weak band occurring in the actual spectrum around the 24-year period has become the principal feature in the whole spectrum of $C(t)$, while the 12-year band in the actual spectrum has become insignificant. The period of the principal line is 23.8 years, but this coarse value, imposed by the discrete frequency step of 1/2048 c/a, will now be refined.

4. The Fundamental Period

The fundamental period of the varve series has been previously taken as approximately 12 years. Just as the 11-year sunspot cycle series derives from a 22-year magnetic cycle, so also the varves could be treated as deriving from a 24 year cycle. We understand clearly that the solar cycle variations in solar ultraviolet radiation, in terrestrial ozone concentration, and in ionospheric electron density, do not reverse when the magnetism reverses. The magnetic

cycle has been rectified before these effects of solar activity are produced, and the same would be true of any variations in varve thickness attributable to the solar cycle. If we allow for the frequency doubling due to rectification, the 12-year period would derive from a double-cycle period in the neighborhood of 24 years. A precise value would be important in case there is a difference between the Precambrian varve period and the modern 11-year sunspot period. A significant difference could have a bearing on the theory of the solar activity cycle, unless of course the solstitial year has changed in 700 million years.

Theoretical reasons have been adduced for thinking that the sunspot period should be lengthening, not shortening (New Scientist, 1987; Noyes et al., 1984) and used against the solar interpretation of the varves. But the deduction is from dynamo theory which has not in fact been established as the cause of the sunspot cycle (Gilman, 1981). On the contrary, the high Q found below presents a new difficulty for relaxation mechanisms such as proposed by the dynamo theory of the solar cycle.

A nominal value of 24.0 years for the carrier period of $C(t)$ results from noting that the first downcross is at year 6 and the last at year 1327, which is 55 downcrosses later. The calculation is sensitive to the two critical zero crossings and does not take the record as a whole into account. The value 24.0 ± 1.75 obtained by Bracewell and Williams (1986) from a histogram of cycle durations defined by zero crossings is, in effect, defined by just the first and last downcrosses.

A different approach would be to locate the centroid of the part of the spectrum in Figure 2(b) that is concentrated in the vicinity of 24 years. As can be seen, the complex of lines is not symmetrical, possibly because of the fluctuations that are characteristic (Bracewell 1986a) of power spectra, but it is evident that a value less than 24 years would result.

The central peaks in the 12-year band of the Sonett and Williams spectrum are at 11.1, 11.5, 11.9, 12.4, and 13 years; they do not sharply indicate a mid-frequency because the peaks are at sum frequencies, arising through rectification, of fine structure in the 24-year band [Figure 2(b)]. This fine structure represents the sidebands that would be expected from the known spectrum (Table II) of the Elatina amplitude modulation, and in the simplest case would consist of peaks spaced at integral multiples of 1/314 c/a.

The 24-year complex is shown to an expanded scale in Figure 7. A string of short ticks straddling the spectrum indicates the expected locations of the eight inner sidebands associated with the Elatina cycle, on the assumption of a carrier of 24 year period with pure amplitude modulation. These ticks are certainly in rough agreement with the spectral features but a much better fit results when the carrier period is adjusted to 23.7 years. The nine vertical arrows rising from the horizontal axis toward the spectral peaks indicate the revised sideband locations; the arrows agree with the peaks better than the sideband

locations based on a 24-year period. Careful consideration suggests that it has been possible to achieve a precision of one decimal, or a fraction of the width of the central line, by involving several lines of the spectrum in the adjustment of the period. For practical use it is believed that a value 23.7 ± 0.2 s.d is justified.

The new precise value for the period of the varve double cycle is longer rather than shorter than the modern magnetic cycle period, but the difference is still less than the standard deviation with which the modern period has been determined.

5. The Q of the Solar Oscillator

The above discussion lifts the $Q = \nu/\Delta\nu$ of the varve oscillator from a value of about 12 (Bracewell and Williams, 1986; Bracewell, 1988) to about 120, a degree of sharpness that works in favour of a clock mechanism (Dicke, 1978; Bracewell, 1988a,c) for solar activity, assuming that the varve thickness was controlled by the sun. Some variants of the relaxation oscillation idea for solar activity will be unable to account for such a high Q. It is true that the theory of the interaction between electrically conducting solar convection currents and magnetic fields in the presence of solar rotation has reached a high pitch of development over many years, but whether the magnetic fields of sunspots can be generated by a self-sustaining convection-rotation dynamo, or whether the convection layer is mainly a propagation medium for the sunspot fields, may now hinge on the ability of dynamo theory to account for high Q oscillation.

When the 12 year period was first reported by Williams it seemed that there might have been a speeding up of the solar cycle over the last 700 million years. However, it was not obvious that the 11 year sunspot period was incompatible with the varve period because each period was at that time associated with a Q of about 7 (Bracewell and Williams, 1986). Thus the difference in periods was only two-thirds of a standard deviation. The present comparison is between 22.2 ± 1.8 and 23.7 ± 0.2. The separation of the periods is still less than one standard deviation and it would be premature to offer explanations for a slowing down of the solar oscillator. Indeed it is possible that further consideration may tend to show that the solar oscillator has changed little over geological time. The evidence from stellar activity cycles, while limited, does not show dependence of stellar cycle period on rotation period (Soderblom and Baliunas, 1988).

6. Explanation of the Actual Spectrum

Return to the peaks at 11.1, 11.5, 11.9, 12.4 and 13 years. Let $f_0 = 1/23.7$ and $\Delta = 1/314$. Peaks in the spectrum of $C(t)$ are expected at $f_0 + n\Delta$ (25.63, 23.70, 22.04, 20.59 years). Corresponding to the various sum frequencies $2f_0 + n\Delta$ we find periods 11.02 ($n = 2$), 11.12 ($n = 1$), 11.85 ($n = 0$), 12.31 ($n = -1$), 12.82 ($n = -2$). Comparing these periods with Table I we see that beating between the carrier and stronger sidebands of the spectrum of $C(t)$ is evidently sufficient to explain the peaks in the 12-year band of Sonett and Williams.

Difference frequencies $n\Delta$ likewise arise from beating; but these frequencies are so low that they combine with the 345-year undulation. Consequently one expects the lowest combination frequencies to have periods 350, 314, 314/2, and $1/(1/314 + 1/350)) = 163$. This expectation agrees with the periods near 333 and 166 years in Table I well within the resolution limit reported.

Consider now the peaks reported with periods of 22.3 (22.3), 24.3 (23.9), and 25.7 (25.6) years; it is true that they are close to the values 22.04, 23.7, and 25.6 calculated above. However, rectification of a sinusoid with period 24, while it would create new periods at 12, 8, 6..., would eliminate the 24-year period. Therefore to explain the 24-year band appearing in the Sonett and Williams analysis it is necessary to invoke an additional phenomenon. One contributing cause is the amplitude modulation but more important is the undulation which, in the presence of rectification, doubles any frequencies $f_0 + n\Delta$ in the intrinsic 24-year band and creates new frequencies at $f_0 + n\Delta + m/T_U$, $m \neq 0$. The low order combinations $(n,m) = (0,1),(-1,1)$, and $(0,-1)$ yield theoretical periods 22.2, 23.9 and 25.4, to be compared with 22.3 (22.3), 24.3 (23.9), and 25.7 (25.6) reported. These numbers are in agreement within a small fraction of the bandwidths tabulated by Sonett and Williams.

It appears then, that all the complexity of the actual spectrum established by Sonett and Williams and presented in the upper part of Figure 2, is contained within the relatively much simpler description presented in the lower spectrum. This advance in understanding has resulted from the meticulous analysis of Sonett and Williams combined with the idea of derectification, the recognition of the undulation so revealed, and the subtraction of the undulation. In retrospect one could say that the complexity seen in the actual spectrum results from applying linear techniques of analysis to a problem embodying essential nonlinearity. This is a satisfactory finding that brings us closer to the physics of the problem and is in the spirit of an earlier attempt at simplification by Sonett (1982).

It is noticeable from Figs. 6 and 7 that there is a continuum underlying the clusters of lines. It has been determined that this continuum arises from a phenomenon that has been reported for both the sunspot and varve series, namely phase modulation (or frequency modulation). Both phase and period have been found to correlate with envelope amplitude, and frequency modulation of the varve series has been put conspicuously in evidence by Sonett and Williams; but delicate analysis is not necessary to demonstrate these effects, which are visible to the eye on the open time scale of Figure 4. Phase modulation broadens any lines, partially fills in the space between lines, and contributes to the lowering of the apparent Q. Consequently it will be necessary to analyze the phase modulation in order to determine the presence of any systematic effect tending to blur the apparent stability of the oscillator which, intrinsically, may prove to possess an even higher Q than appears now.

10

7. Third Harmonic in the Intrinsic Spectrum

A broad band centered on 8 years represents third harmonic of the frequencies in the 24-year band. The third harmonic arises from a phenomenon that has been explored in detail in connection with sunspots (Bracewell 1988u). When a sunspot semicycle is strong, its shape departs from sinusoidal in the direction of being triangular; in other words, the profile is sharpened. It is true that, in the case of a strictly periodic waveform, this change in shape is producible by adding third harmonic (period $\sim$ 8 years) to a sinusoidal fundamental. Consequently it is not surprising that third harmonic appears in the spectrum of $C(t)$, which after all is quasiperiodic. However, the "third harmonic" appears as a band around 8 years rather than as a sharp line, because it is contributed to only by some semicycles (the strong ones) and at periods ranging from 6 to 10 years in accordance with the variation in semicycle duration.

The sharp semicycles pointed out above in connection with Figure 4 show that the nonlinearity responsible also affects the varves, as it should if the sun controlled the varve thickness. The cause of the sharpening (Bracewell, 1985) of the semicycle shape has now been attributed to an empirically determined nonlinear three-halves law. The discovery of this law led to the realization that it arises from the sunspot number definition (Bracewell 1988b); large sunspot groups, being emphasized in proportion to their duration, enhance the sunspot number when the latter is large. If sunspots were due to an underlying physical influence that varied strictly sinusoidally in time then, despite the monochromatism, the nonlinearity built into the sunspot definition would give rise to the appearance of third harmonic in the sunspot number series. A reasonable approach to the nonlinearity would be to correct for it before performing spectral analysis. The spectrum of $C(t)$ would then be even further simplified, consisting mainly of a 24-year fundamental with the sidebands arising from the Elatina cycle envelope.

8. Physical Interpretation of the Intrinsic Spectrum

The 24-year multiplet of Figure 2(b), comprising a carrier and several sidebands, could in principle be attributed entirely to the oscillator. However, it suffices to invoke a monochromatic oscillator, because sidebands would be generated as the cyclic influence was transmitted to the surface. For example, if the transmission mechanism were wave propagation, frequency modulation would be imposed by a moving medium such as the convection layer, circulation times of the order of centuries being indicated. Likewise amplitude modulation would result from propagation through the inhomogeneous solar medium because of interference between direct and indirect rays. A synthesis of the spectrum from ray theory will be presented separately.

9. Discussion

11

In the hope of understanding, or merely predicting, sunspot activity, authors have created an extensive literature of numerical analysis of the sunspot number series, but progress hitherto has been essentially of a descriptive kind. The discovery of the varves in the Elatina formation at Pichi Richi Pass by Dr. G.E. Williams has completely altered things. The simple fact that the geological varve series is much longer than the sunspot series has made it possible to describe the solar activity oscillation in an economical way. Much previous complication has been cleared and the remaining step to physical interpretation has been reduced. Artificial nonlinearities standing between the physical quantity that oscillates and the recorded appearances have been removed to give a glimpse of an underlying quasimonochromatic source.

This development affects two main topics in solar physics: self-sustaining dynamo action associated with the convection layer and solar rotation, and the theory of nuclear power generation. That part of dynamo theory which is concerned with providing a convection-rotation source for the solar cycle has not reached consensus (Piddington, 1975, 1978, Gilman, 1981), which becomes understandable if the source is below the convection layer (Layzer et al., 1979). Likewise, solar energy theory, even though mature, may benefit from modification as to the composition of the core. If the sun has an oscillating inert core, then neutrino production would be less than currently calculated, because less power would be produced by fusion of hydrogen into helium and more by the CNO cycle of reactions (Bracewell, 1988c). This is important because standard theory overestimates neutrino production by 7.9/2.0 and ways of modifying the theory are being sought.

There is reason to believe that in a sun born from a cosmic mix of hydrogen, helium and trace elements, iron in cosmic abundance would be soluble in the hydrogenic plasma (Iyetomi and Ichimaru, 1986). However, prior sedimentation in the protosolar nebula has been considered (Prentice, 1983) as a mechanism for a heavy-element inert solar core; heavy-element cometary nuclei, rare today, may have been an important component of the protosolar nebula (Prentice, 1986; Bailey et al., 1986); and there is a dynamical argument calling for iron and silicate-derived cores in the major planets and the sun (Cole, 1987). If comets, or cometesimals (Donohue et al., 1987), became an important constituent of the interstellar medium after the first generation of supernovae contributed both heavy elements and ready-formed grains such as silicon carbide, then the second generation stars would have cores. The whole theory of the internal constitution of the stars would then require revision.

The varve discovery will also affect astrophysics to the extent that the dozens of stars now evidencing stellar activity cycles, and star formation in general, may depend for elucidation on progress in understanding solar activity.

It is intriguing to see that fundamental problems of astrophysics are being affected by the geological discovery of G.E. Williams and to consider that other fossil records are certain to exist and that they will contribute to the development of a new resource for astrophysics.

Acknowledgments

References

Bracewell, R.N.: 1953, *Nature*, 171, 649.

Bracewell, R.N.: 1985, *Aust. J. Phys.*, 38, 1009.

Bracewell, R.N.: 1986a, *The Fourier Transform and Its Applications*, (second ed. revised), McGraw-Hill, New York.

Bracewell, R.N.: 1986c, *Nature*, 323, 516.

Bracewell, R.N.: 1986b, *The Hartley Transform*, Oxford University Press, New York.

Bracewell, R.N.: 1988a, *Solar Phys.*, (in press).

Bracewell, R.N.: 1988b, *Mon. Not. Roy. Astron. Soc.*, (in press).

Bracewell, R.N.: 1988c, *Quarterly J. Roy. Astron. Soc.*, (in press).

Bracewell, R.N. and Williams, G.E.: 1986, *Mon. Not. Roy. Astron. Soc.*, 223, 457.

Bailey, M.E., Clube, S.V.M., and Napier, W.M.: 1986, *Vistas in Astronomy*, 29, 53.

Cole, G.H.A.: 1987, private communication.

Cole, T.W.: 1973, *Solar Phys.*, 30, 103.

Dicke, R.H.: 1978, *Nature*, 276, 676.

Donahue, T.M., Gombosi, T.I., and Sandel, B.R.: 1987, *Nature*, 330, 548.

Gilman, P.A.: 1981, 'Global Circulation and the Solar Dynamo,' chapter in *The Sun as a Star*, NASA SP-450, p.231.

Iyetomi, H. and Ichimaru, S.: 1986, *Phys. Rev. A*, 34, 3203.

Layzer, D., Rosner, P. and Doyle, H.T.: 1979, *Astrophys. J.*, 229, 1126.

Noyes, R.W., Weiss, N.O., and Vaughan, A.H.: 1984, *Astrophys. J.*, 287, 769.

New Scientist, 22 October 1987, p.34.

Piddington, J.H.: 1975, *Astrophys. and Space Sci.*, 38, 157.

Piddington, J.H.: 1978, *Astrophys. and Space Sci.*, 55, 401.

Prentice, A.J.R.: 1983, *Proc. Astronom. Soc. Aust.*, 5, 183.

Prentice, A.J.R.: 1986, *Proc. Astronom. Soc. Aust.*, 6, 394.

Soderblom, D.R. and Baliunas, S.L.: 1988, in F.R. Stephenson and J.A. Eddy (ed.), 'The Sun Among the Stars.' *Secular Solar and Geomagnetic Variations in the Last 10,000 Years*, Reidel, Dordrecht.

Sonett, C.P. and Williams, G.E.: 1987, *Solar Physics*, 110, 397.

Sonett, C.P.: 1982, *Geophys. Res. Letters*, 9, 1313.

Williams, G.E.: 1981, *Nature*, 291, 624.

Williams, G.E.: 1983, in B.M. McCormac (ed.), 'Precambrian Varves and Sunspot Cycles.' *Weather and Climate Responses to Solar Variations*, Colorado Assoc. Universities Press, Boulder, p. 517.

Williams, G.E.: 1985, *Aust. J. Phys.*, 28, 1027.

Williams, G.E.: 1986, *Scientific American*, 255, no. 2, 88.

Williams, G.E.: 1987, *New Scientist*, 25 June 1987, p. 63.

Williams, G.E. and Sonett, C.P.: 1985, *Nature*, 318, 523.

Williams, G.E. and Tonkin, D.G. 1986, *Aust. J. Earth Phys.*, 32, 287.

Zahnle, K.J. and Walker, J.C.G.: 1987, *Climatic Change*, 10, 269.

TABLE AND FIGURE CAPTIONS

Table I. Spectral peaks found in the upper and lower halves of the varve-thickness series by Sonett and Williams (1987).

Table II. Fourier coefficients for the Elatina modulation envelope $E_E(t)$.

Table III. Spectral peaks of $C(t)$.

Figure 1. Varve thickness $V(t)$ in mm versus varve serial number or "varve year."

Figure 2. (a) The two varve spectra found by Sonett and Williams after dividing the data $V(t)$ into upper and lower halves, (b) the simpler spectrum of the centralized waveform $C(t)$ prepared by derectification. The numerous spectral lines above prove to be derivable from the simpler spectrum below.
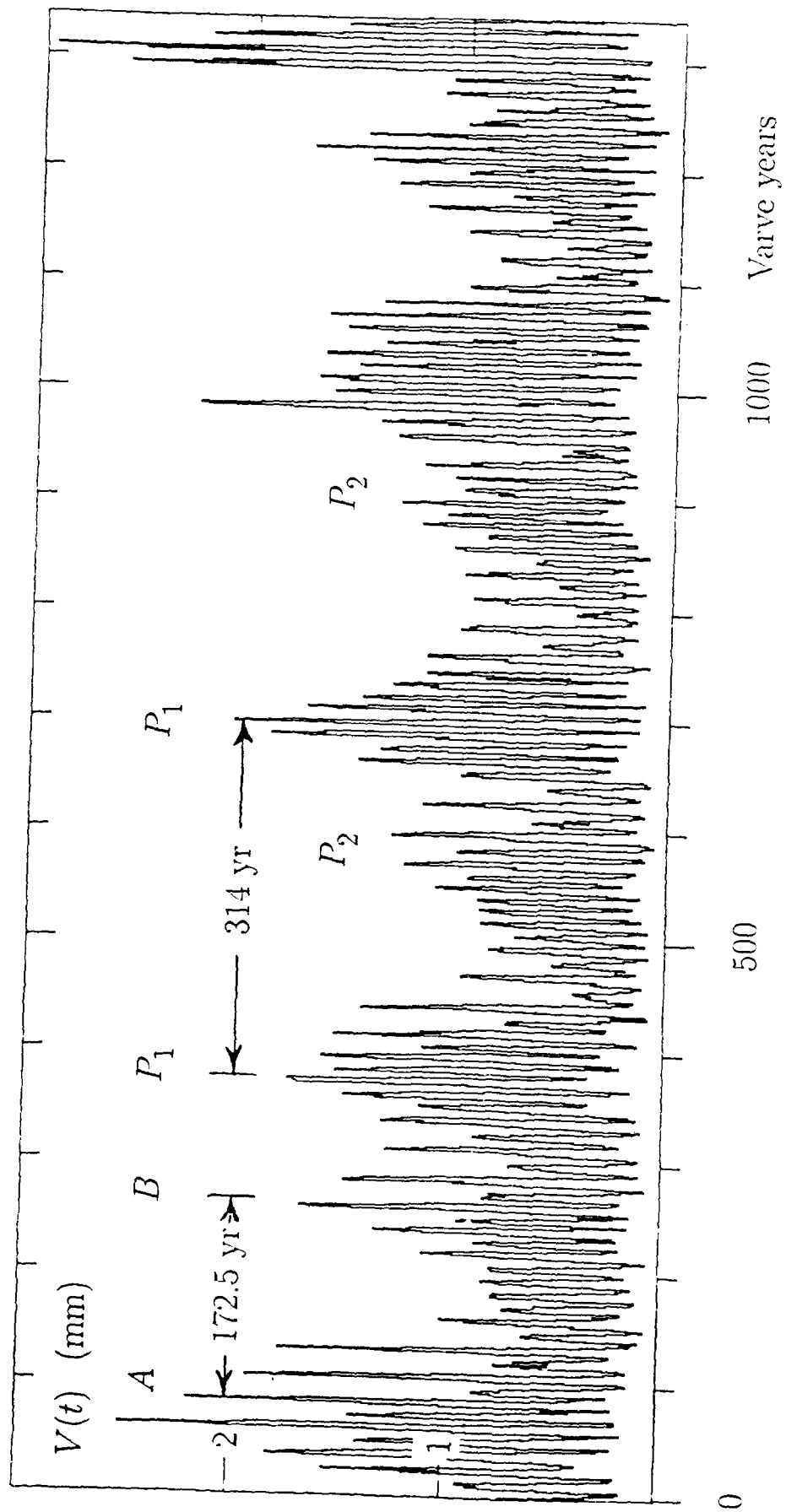
Figure 3. Showing how zig-zag effect, with a period $T_U = 345$ years (below) arises by rectification of an alternating quantity $\sin(2\pi t/23.7)$ superimposed on an undulation $U \sin(2\pi t/345)$ that is relatively weak ($U < 1$). The scale markers, set to agree with the strong peaks at the first episode of unequal cycles (A), show how a role reversal sets in for the following episode (B).

Figure 4. The centralized undulation-free oscillation $C(t)$ prepared from $V(t)$, clearly exhibiting the Elatina cycle modulation, whose peaks (P_1, P_2) and minima (M_1, M_2) are aligned vertically. The 345 year undulation has been subtracted but has left its trace in the form of semicycles sharpened by a nonlinear dependence of varve thickness on the solar cycle oscillation. Ordinates are normalized to a maximum absolute value of unity (at year 1307). The abscissa is varve year measured from origins at 0, 314, 628, and 942 in successive lines.

Figure 5. One period of the mean amplitude-modulating envelope $E_E(t)$ that characterizes the 314 year Elatina cycle.

Figure 6. The complete amplitude spectrum of the centered undulation-free varve series $C(t)$. Note the absence of components at and around zero frequency, the faintness of the 12-year feature, and the weak band around 8 years.

Figure 7. The low frequency part of the spectrum of $C(t)$. Vertical arrows show the computed location of sidebands of a 23.7 year oscillation subject to pure amplitude modulation with a period of 314 years. Vertical ticks straddling the spectrum and referring to a 24.0 year oscillation, do not fit the peaks as well.
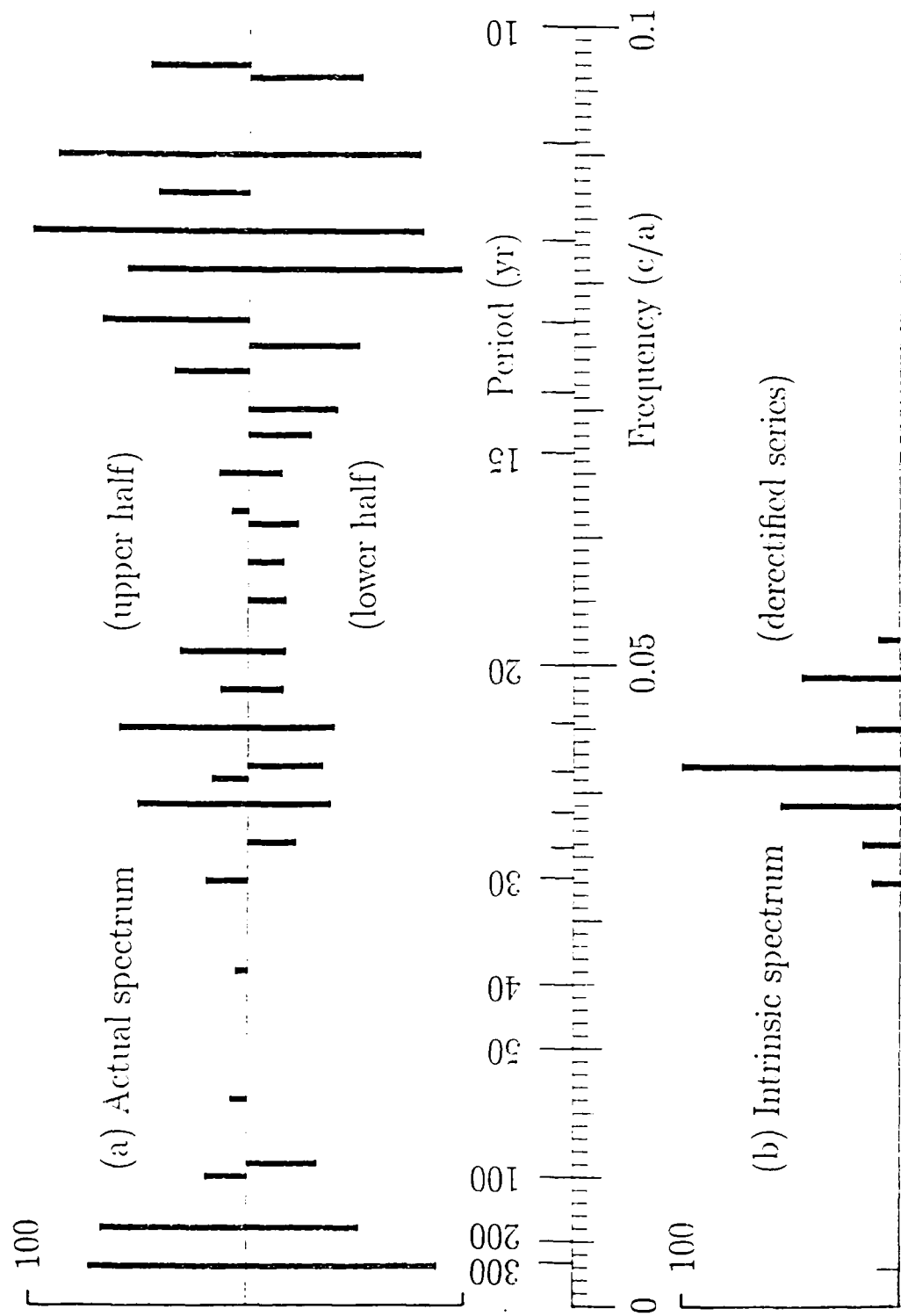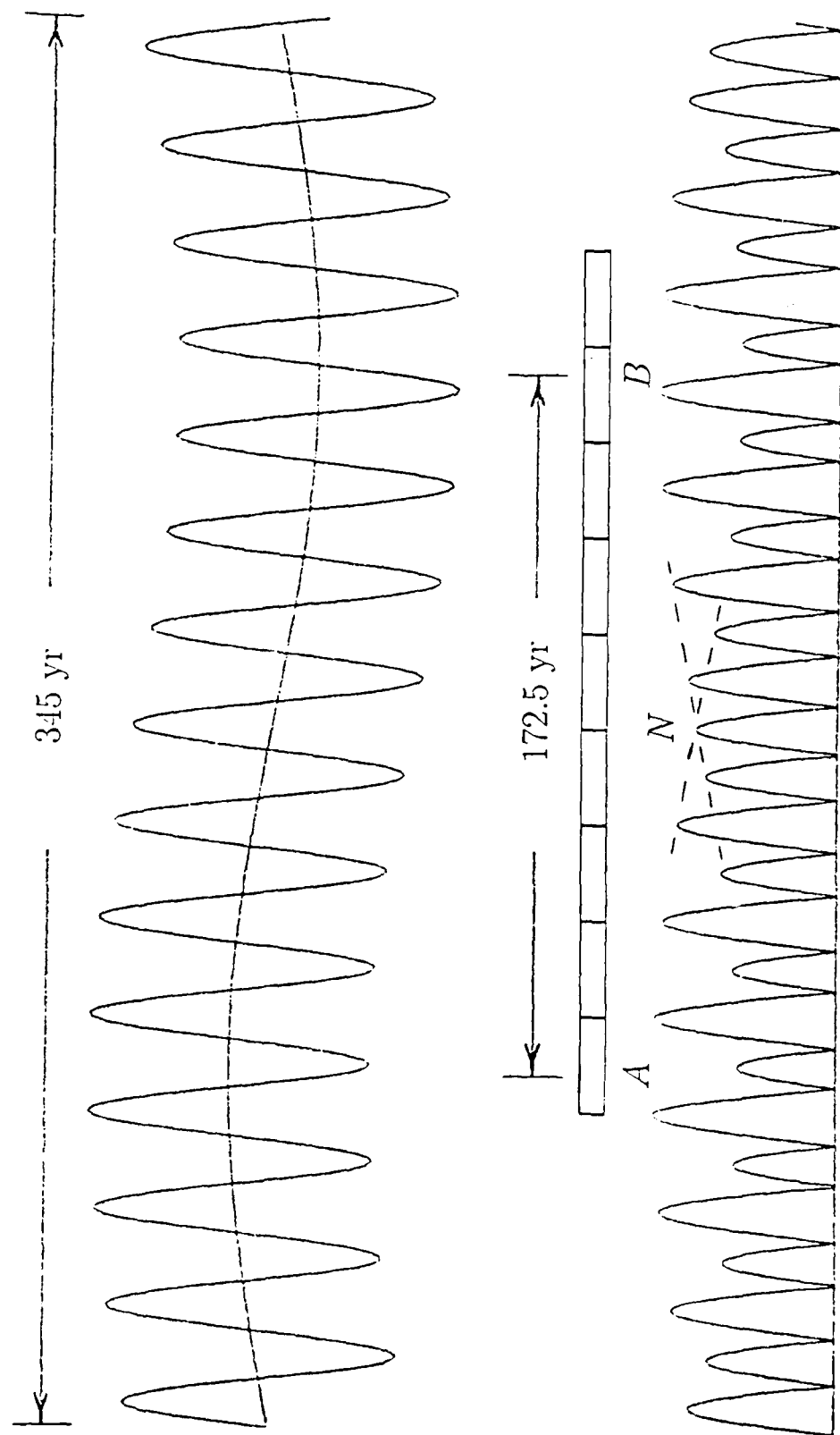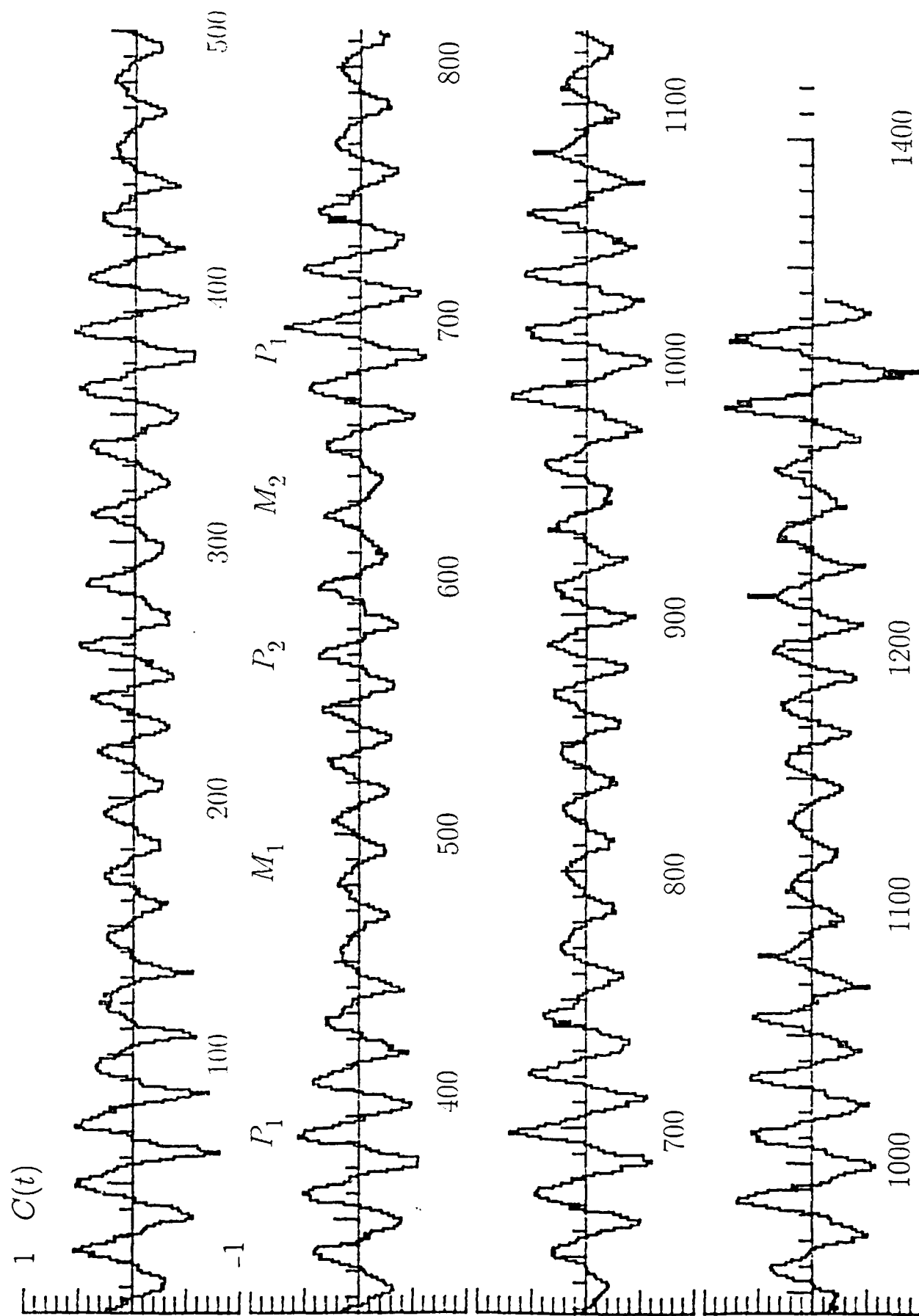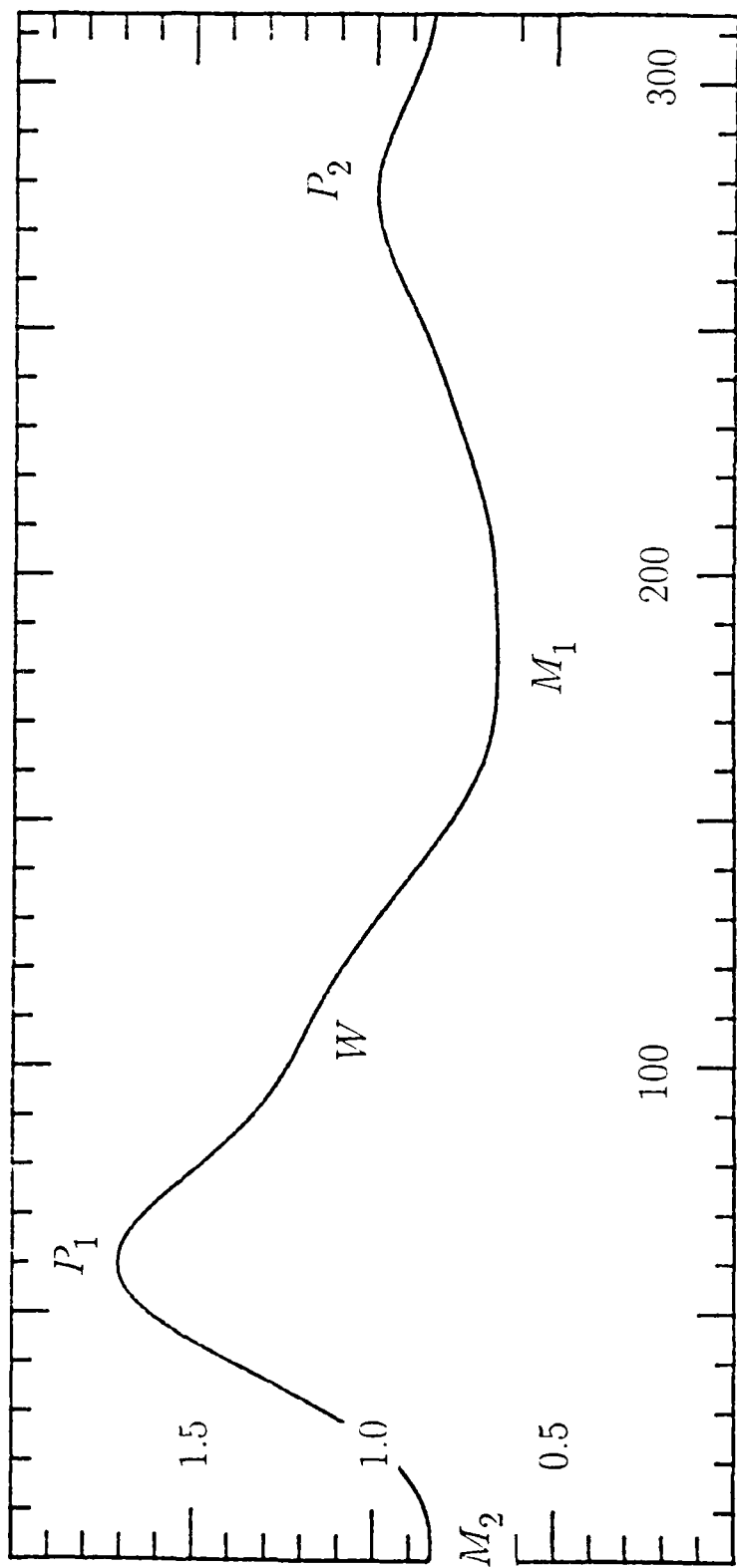
15

Fig. 1

Fig. 2

Period (yr)

Frequency (c/a)

(upper half)

(lower half)

10   0.1

15

20   0.05

30

40

50

100

200

300

100

0

100

(a) Actual spectrum

(b) Intrinsic spectrum

(derectified series)

Fig. 3

$C(t)$

1

-1

P_1

M_1

P_2

M_2

P_1

100 200 300 400 500

400 500 600 700 800

700 800 900 1000 1100

1000 1100 1200 1300 1400

P_1

P_2

W

M_1

M_2

1.5

1.0

0.5

100

200

300

Fig. 6

Fig. 7